University of Groningen

The characteristics of pallidal low-frequency and beta bursts could help implementing adaptive brain stimulation in the parkinsonian and dystonic internal globus pallidus

Pina-Fuentes, Dan; van Zijl, Jonathan C.; van Dijk, J. Marc C.; Little, Simon; Tinkhauser, Gerd; Oterdoom, D. L. Marinus; Tijssen, Marina A. J.; Beudel, Martijn

IMPORTANT NOTE: You are advised to consult the publisher's version (publisher's PDF) if you wish to cite from it. Please check the document version below.

Document Version
Publisher's PDF, also known as Version of record

[Link to publication in University of Groningen/UMCG research database](#)

The characteristics of pallidal low-frequency and beta bursts could help implementing adaptive brain stimulation in the parkinsonian and dystonic internal globus pallidus
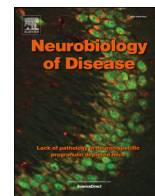
Dan Piña-Fuentes[a,b,1], Jonathan C. van Zijl[a,b,1], J. Marc C. van Dijk[a], Simon Little[c], Gerd Tinkhauser[d,e], D.L. Marinus Oterdoom[a], Marina A.J. Tijssen[b], Martijn Beudel[b,f,*]

[a] *Department of Neurosurgery, University Medical Center Groningen, University of Groningen, Groningen, The Netherlands*
[b] *Department of Neurology, University Medical Center Groningen, University of Groningen, Groningen, The Netherlands*
[c] *Sobell Department of Motor Neuroscience and Movement Disorders, Institute of Neurology, Queen Square, London, UK*
[d] *Medical Research Council Brain Network Dynamics Unit and Nuffield Department of Clinical Neurosciences, University of Oxford, United Kingdom*
[e] *Department of Neurology, Bern University Hospital and University of Bern, Bern, Switzerland*
[f] *Department of Neurology, Isala Clinics, Zwolle, The Netherlands*

ARTICLE INFO

ABSTRACT

Introduction: Adaptive deep brain stimulation (aDBS) has been applied in Parkinson's disease (PD), based on the presence of brief high-amplitude beta (13–35 Hz) oscillation bursts in the subthalamic nucleus (STN), which correlate with symptom severity. Analogously, average low-frequency (LF) oscillatory power (4–12 Hz) in the internal globus pallidus (GPi) correlates with dystonic symptoms and might be a suitable physiomarker for aDBS in dystonia. Characterization of pallidal bursts could facilitate the implementation of aDBS in the GPi of PD and dystonia patients.
Objective and methods: We aimed to describe the bursting behaviour of LF and beta oscillations in a cohort of five GPi-DBS PD patients and compare their amplitude and length with those of a cohort of seven GPi-DBS dystonia, and six STN-DBS PD patients (n electrodes = 34). Furthermore, we used the information obtained to set up aDBS and test it in the GPi of both a dystonia and a PD patient (n = 2), using either LF (dystonia) or beta oscillations (PD) as feedback signals.
Results: LF and beta oscillations in the dystonic and parkinsonian GPi occur as phasic, short-lived bursts, similarly to the parkinsonian STN. The amplitude profile of such bursts, however, differed significantly. Dystonia showed higher LF burst amplitudes, while PD presented higher beta burst amplitudes. Burst characteristics in the parkinsonian GPi and STN were similar. Furthermore, aDBS applied in the GPi was feasible and well tolerated in both diseases.
Conclusion: Pallidal LF and beta burst amplitudes have different characteristics in PD and dystonia. The presence of increased burst amplitudes could be employed as feedback for GPi-aDBS.

1. Introduction

The internal part of the globus pallidus (GPi) is currently the preferred target for conventional (continuous) deep brain stimulation (cDBS) in dystonia (Balint and Bhatia, 2014) and one of the two main targets for cDBS in Parkinson's disease (PD), together with the subthalamic nucleus (STN)(Odekerken et al., 2016). In both diseases, patients show a significant improvement after cDBS implantation, being

around 30% improved in the Unified PD Rating Scale (UPDRS) part III in PD and demonstrating a motor and disability improvement up to 60% in isolated dystonia (Moro et al., 2017). However, despite its clear clinical benefit, cDBS still has some limitations. cDBS programming can be troublesome and time-consuming, especially in dystonia, in which a visible clinical response is usually delayed for weeks or months, and the overall response across dystonia subtypes to cDBS can be limited and difficult to predict (Picillo et al., 2016). Furthermore, side effects such

Table 1

Clinical information of PD and dystonia patients. Pt = patient, PD = Parkinson's disease, Dys = dystonia, GPi = internal globus pallidus, STN = subthalamic nucleus M = male, F = female, y = years, aDBS = adaptive deep brain stimulation, UPDRS = Unified Parkinson's Disease Rating Scale, LDED = levodopa daily equivalent dose, DBS = deep brain stimulation, R = right, L = left. †Clinical score after 1 year of DBS implantation.

Pt	Age	Sex	PD type	Disease duration (y)	Type of surgery	ON/OFF UPDRS PART III	Most affected side	Medication	Medical history of dystonia
PD-GPi 1	65	M	Akinetic-Rigid	25	Battery replacement		Right	Levodopa, amantadine 1200 mg LDED	No
PD-GPi 2	54	M	Akinetic-Rigid	8	New implantation	38/12	Left	Levodopa, entacapone 750 mg LDED	Yes. Peak-dose dystonia
PD-GPi 3	64	F	Akinetic-Rigid	23	Battery replacement		Left	Duodopa, amantadine 1759 mg LDED	Yes. Dystonic hand.
PD-GPi 4	64	M	Akinetic-Rigid	11	New implantation	29/11	Right	Levodopa, ropinirole, amantadine 1190 mg LDED	Yes. Cervical dystonia
PD-GPi 5 (aDBS)	58	F	Tremor	14	Battery replacement		Right	Levodopa, pramipexole, amantadine 1175 mg LDED	Yes (early morning dystonia)
PD-STN 1	71	F	Akinetic-Rigid	8	New implantation	31/11	Left	Levodopa, pramipexole 844 mg LDED	No
PD-STN 2	73	M	Akinetic-Rigid	17	New implantation	57/40	Right	Levodopa, apomorphine 2569 mg LDED	Yes. Biphasic dystonia
PD-STN 3	70	M	Akinetic-Rigid	10	New implantation	37/17	Right	Levodopa, ropinirole 1098 LDED	Yes (big toe)
PD-STN 4	47	F	Akinetic-Rigid	8	New implantation	38/14	Right	Levodopa, amantadine, apomorphine 651 mg LDED	No
PD-STN 5	55	M	Tremor	5	New implantation	46/20	Right	Levodopa, pramipexole, apomorphine 1808 mg LDED	Yes (torticollis)
PD-STN 6	59	F	Akinetic-Rigid	10	New implantation	19/6	Right	Levodopa, rotigotine, seleginine 1710 mg LDED	No

Pt.	Age	Sex	Dystonia type	Disease duration (y)	Type of surgery	BFMDRS PRE/POST†	TWSTRS PRE/POST†	Etiology	Medication	Clinical presence of phasic dystonia
Dys-GPi 1	47	M	Generalized (secondary) + spastic hemiparesis	11	New implantation	49/53		Prob. Perinatal hypoxia	Lorazepam	Yes. Distonic tremor
Dys-GPi 2	52	M	Segmental dystonia (torticollis)	3	New implantation	23/14.25		-	Clonazepam	Yes. Jerks, dystonic tremor. Improvement with Sensory trick.
Dys-GPi 3	52	F	Segmental dystonia (Myoclonus-dystonia)	33	New implantation	25.25/12	22.5/17.5	-	Propranolol, zolpidem	Yes. Improvement with sensory trick
Dys-GPi 4	63	M	Cervical dystonia	20	New implantation	19.5/11.25	16.5/13.5	-	Clonazepam	Yes
Dys-GPi 5	63	M	Segmental dystonia (torticollis and oromandibular) + Holmes tremor	63	New implantation	13.75/5	20/8.5	Prob. Perinatal hypoxia	Clonazepam	Yes
Dys-GPi 6	65	F	Segmental dystonia (torticollis)	12	New implantation	15.25/12	22/13	-	-	Yes, dystonic tremor
Dys-GPi 7 (aDBS)	65	F	Blepharospasm and oromandibular dystonia (Meige's syndrome)	9	Battery replacement			-	Botulinum toxin every 10 weeks	Yes

as dystonia / dyskinesias (in PD), parkinsonism (in dystonia) or dysarthria (in both conditions) may occur (Odekerken et al., 2016; Vidailhet et al., 2013).

With the aim of improving efficacy and limiting side effects, *adaptive* DBS (aDBS) systems which only stimulate when pathological neural activity and/or clinical symptoms are present are currently being explored (Beudel and Brown, 2016). Preliminary evidence shows that this new DBS technique is at least as efficacious as cDBS (Arlotti et al., 2018; Little et al., 2013; Piña-Fuentes et al., 2017), whereas aDBS may induce fewer side effects and reduce energy consumption (Little et al., 2016; Rosa et al., 2017). In PD, this adaptive form of DBS is based on the level of exaggerated beta (13–35 Hz) oscillations in the STN, which have been correlated with contralateral parkinsonian symptoms (Neumann et al., 2016). Beta oscillations occur in phasic bursts (Little et al., 2013), and the characteristics of those bursts are reactive to treatment response. Specifically, their amplitude and duration positively correlate with clinical symptoms, and a reduction on both parameters is seen after levodopa (Tinkhauser et al., 2017b) and aDBS (Tinkhauser et al., 2017a) (but only a reduction in amplitude in cDBS). Moreover, the coefficient of variation (CoV) of beta oscillations —an indicator of the variability of a signal over time— is negatively correlated with the severity of parkinsonian symptoms, and increases after levodopa administration (Little et al., 2012). Such dynamic properties of beta oscillations have made it possible to implement them as physiomarker in aDBS (Arlotti et al., 2018). These exaggerated oscillations are not only restricted to the STN, but also prominently present in the GPi of PD patients (Jimenez-Shahed et al., 2016; Silberstein et al., 2003; Tsiokos et al., 2017) and they are synchronized between nuclei when measured simultaneously (Brown et al., 2001). This phenomenon indicates a general pathological oscillatory status within the basal ganglia circuitry (Chiken and Nambu, 2016).

Analogously, a prominent pallidal low-frequency (LF; ± 4–12 Hz) oscillatory activity has been reported across many dystonia subtypes (Piña-Fuentes et al., 2018). Early studies revealed that an increased musculo-muscular dystonic drive in the theta (4–7 Hz) band was present in cervical dystonia (Tijssen et al., 2000), as well as a correlation of LF oscillations in the GPi with multi-unit neuronal activity and dystonic electromyogram (EMG) periods (Chen et al., 2006; Chu Chen et al., 2006). LF oscillations in the GPi have been shown to be especially coherent with EMG phasic dystonic components (Liu et al., 2006). Prominent LF oscillations in dystonia have been also found at a single-unit level of GPi microelectrode recordings (Starr et al., 2005). Further evidence for a role of GPi-LF power in dystonia comes from EMG and intra-operative local field potential (LFP) recordings, which showed that LF power and coherence are suppressed by DBS and that their rate of suppression correlates with the improvement of the phasic components of dystonia (Barow et al., 2014; Foncke et al., 2007; Neumann et al., 2017; Wang et al., 2018). In contrast, evidence of prominent LF oscillations in the STN of dystonia patients is scarce, mostly due to the fact that the GPi —and not the STN, is the preferred target for DBS in dystonia. From the two research groups that reported STN-LFPs in dystonia, one found more prominent STN-LF oscillations in dystonia compared to PD (Geng et al., 2017), while the other did not (Wang et al., 2016).

Oscillatory LF and beta pallidal power has been mostly determined by means of power spectral density (PSD) estimates. As PSD estimates only represent the average oscillatory power, understanding the properties of the parkinsonian and dystonic GPi bursts could provide further evidence of the behavior of oscillatory networks over time on each disease and allow aDBS algorithms to be implemented also in the GPi according to the physiomarker selected. In this study, we aimed to compare the burst characteristics of the dystonic and parkinsonian GPi, and the parkinsonian GPi versus the parkinsonian STN. This was performed with the goal of determining similarities or differences between diseases, or between different nuclei in the same disease. In addition, as a proof of principle, we tested aDBS in the GPi of both a dystonia and a

PD patient.

2. Materials & methods

2.1. Patients

Eleven patients with PD and seven patients with dystonia who underwent either DBS placement or battery replacement surgery in the University Medical Center Groningen, the Netherlands, participated in this study (Table 1). All patients gave written informed consent to the study protocol, which was approved by the local ethical committee. Five PD patients (8 electrodes) and all dystonia patients (14 electrodes) were measured in the GPi, whereas six PD patients (12 electrodes) were measured in the STN. Either dopaminergic or anti-dystonic medication were suspended for least 12 h prior to the measurements.

2.2. Resting state recordings

2.2.1. Data acquisition

Intraoperative LFPs were bilaterally recorded from two quadripolar DBS electrodes (Medtronic lead model 3387/3389), while patients were in a supine resting state for approximately 90 s, using a sampling rate of 1000 Hz, except in two GPi-PD patients in which the recordings were unilateral (i.e. the first patient had only one side implanted in the GPi and a technical problem with the second patient caused that no signal could be registered on one of the electrodes). Recordings were initially performed either using a monopolar montage, and nasion-referenced using a EEG/PSG headbox, (SleepRT. Rumst, Belgium), or a bipolar montage, using contacts 0–2 and 1–3 for each DBS lead (Spike2 Version 8, Cambridge Electronic Design, Cambridge, United Kingdom). Signals were amplified, and bandpass filtered at 1–500 Hz (BrainRT™ software) for monopolar recordings and 3–37 Hz for bipolar recordings.

2.2.2. Signal processing

LFPs were analyzed offline using MATLAB (ver. 2018a, Mathworks,Inc. Natick, Massachusetts, USA) and FieldTrip toolbox (Donders Center for Cognitive Neuroimaging, University Nijmegen, Nijmegen, the Netherlands). Monopolar channels were filtered (bandpass at 4–35 Hz) and visually inspected, in order to select the largest segment without artifacts. Segments of 45s were selected for further analysis for each channel. Monopolar LFPs were re-referenced using a bipolar montage. Remaining jump (~0–2 per recording) and electro-cardiographic (ECG, 1 patient) artifacts were suppressed by means of a wavelet denoising filter (Taswell, 2000) (example shown in Supplementary Fig. 1). Signals were passed through a denoising filter with a sym4 wavelet, using a Bayes method with 10 levels and a soft (jump) or hard (ECG) threshold, with subsequent subtraction of the result from the original signal. Artifact suppression (instead of rejection) was necessary, as continuity of the recording is essential for burst analysis. Cutting out remaining artifacts and attaching the rest of the recording would have induced artificial waveforms and broken such continuity. Additionally, subharmonic powerline noise at 24 Hz was suppressed by averaging the power of adjacent frequency bands using a symmetric nearest neighbor filter. Each bipolar channel was normalized to its root mean square (RMS) value to account for differences in voltage gains, and amplitude was expressed as arbitrary units (a.u.).

2.2.3. Power spectral density (PSD)

Individual PSD estimates were obtained using Welch's method with segments of 2000 discrete Fourier transform points and 50% overlap, and smoothed using a moving average filter. The channel per hemisphere that presented the highest combined LF-beta power (highest area under the 4–35 Hz band calculated by integration using a trapezoidal method) was selected for further analysis. The resulting PSD estimates for each group were selected for statistical analysis, using the values of PSD bins of 0.5 Hz between 4 and 35 Hz (Table 2).

Table 2
Peaks per contact in the low frequency and beta band for the selected bipolar LFPs per hemisphere in dystonia and PD. PD = Parkinson's disease, Dys = dystonia, GPi = internal globus pallidus, STN = subthalamic nucleus, SEM = standard error of the mean, LF = low-frequency, freq = frequency.

Patient	Side	Contact selected	Highest LF peak (Hz)	Highest beta peak (Hz)
PD-GPi 01	Right	0–2	10.5	18.5
	Left	0–2	7	14
PD-GPi 02	Left	1–3	9	18
PD-GPi 03	Right	0–2	5.5	28.5
PD-GPi 04	Right	1–3	7.5	15
	Left	1–3	7.5	16
PD-GPi 05	Right	1–3	8	19.5
	Left	0–2	7	18.5
Mean freq Peak (± SEM)			7.7(0.5)	18.3(2.1)
Dys-GPi 01	Right	0–1	11.5	18.5
	Left	2–3	11	16
Dys-GPi 02	Right	0–1	5(7)	24
	Left	0–1	5(7)	23
Dys-GPi 03	Right	1–2	5(7)	14.5
	Left	1–2	8	15
Dys-GPi 04	Right	0–1	6(7)	20
	Left	0–1	12	19
Dys-GPi 05	Right	0–1	10	14.5
	Left	2–3	10	18.5
Dys-GPi 06	Right	2–3	5.5(7)	19.5
	Left	0–1	7.5	22.5
Dys-GPi 07	Right	0–2	10	17
	Left	0–2	10	20.5
Mean freq Peak (± SEM)			8.5(0.7)	18.7(0.8)
PD-STN 01	Right	1–2	11	16
	Left	2–3	12	17.5
PD-STN 02	Right	0–2	8	17.5
	Left	0–2	8	15.5
PD-STN 03	Right	2–3	6(7)	18
	Left	2–3	7	14.5
PD-STN 04	Right	1–2	6.5(7)	27
	Left	1–2	8.5	27
PD-STN 05	Right	0–1	6.5(7)	29
	Left	1–2	6.5(7)	28.5
PD-STN 06	Right	1–2	9.5	19
	Left	2–3	9	17.5
Mean freq Peak (± SEM)			8.7(0.8)	22.6(2.2)

2.2.4. Coefficient of variation (CoV)

To obtain the CoV of each bipolar channel, a continuous wavelet transformation was performed on the selected LFPs using Morlet wavelets, with a sampling frequency of 1000 Hz to perform the appropriate scale-to-frequency conversions (45 s = 45000 values per frequency bin and 140 scaled frequency bins). Afterwards, the CoV was calculated by dividing the standard deviation (SD) of each frequency bin over the mean value of the corresponding bin. CoV values were averaged in four frequency bands (theta 4–8 Hz; alpha 8–12 Hz; low-beta 13–20 Hz; and high beta 21–30 Hz) and used for statistical analysis.

2.2.5. Burst analyses

Normalized bipolar LFPs were re-filtered around the highest peak ± 3 Hz in the LF and beta range. If the peak was < 7 Hz, the LFP was bandpass-filtered around 7 Hz. Also, peaks at the edge of the LF/ beta transition were allowed to include frequencies of the opposite band only if a peak of the opposite band was not included on the ± 3 Hz range. This resulted in two peak-filtered LFPs per bipolar LFP processed, one around the low-frequency peak and one around the beta peak. As each filtered LFP contained amplitude values oscillating around zero (both positive and negative), the amplitude envelope of the filtered signal was calculated, which depicts the overall magnitude

(absolute values) of the oscillatory activity. The amplitude envelope of each filtered LFP was obtained by calculating the modulus of the analytical signal after applying a Hilbert transformation to the filtered LFP (68 amplitude envelopes in total) (Fig. 1).

Bursts were calculated for every amplitude envelope by selecting a percentile value of the total envelope as a threshold, according to Tinkhauser et al., 2017a, 2017b(50th, 55th, 60th, 65th, 70th,75th,80th, 85th, and 90th percentile); individual bursts per amplitude envelope were then defined as the amount of time that the amplitude envelope remained above the selected threshold, from the moment the amplitude exceeded the critical value until the amplitude went down below such value. Burst amplitude was calculated by subtracting the maximum amplitude of every burst to the critical value of the threshold selected. Burst length was calculated as the amount of time each individual burst lasted, measured in milliseconds. Burst duration and amplitude were further divided in 9 arbitrary categories of equal intervals per condition (< 0.2 to ≥0.16 a.u. in steps of 0.2 a.u. for LF amplitude, < 0.1 to ≥ 0.8 a.u. in steps of 0.1 a.u. for beta amplitude, and 100 to ≥ 500 ms in steps of 50 ms for burst duration), in order to visualize progressive transitions between low and high values. The amount of bursts present in each category were further expressed as percentages of the total amount of bursts of each amplitude envelope. Moreover, the total amount of bursts from the Dystonia-GPi and PD-GPi amplitude envelopes were pooled and divided into quartiles. Each burst was then assigned into an amplitude quartile and a length quartile. The same procedure was repeated for the PD-GPi and PD-STN bursts.

2.3. aDBS recordings

2.3.1. Data acquisition aDBS

Additionally, aDBS was tested on both the last Dystonia-GPi and PD-GPi patients (Dys-GPi7 and PD-GPi5). Bilateral recordings were performed using a custom-made amplifier (Little et al., 2016) and script, either from the contacts 0–2 or 1–3, while stimulation was administered using contacts 1 or 2, respectively. Three conditions —namely no stimulation (NoStim), cDBS and aDBS, were applied while the patient was in a supine resting state, at a frequency of 135 Hz and with a pulse width of 60 μs. Prior to the trials, a brief (± 30 s) recording was performed from both the upper and lower contact pairs, with the LFPs bandpass filtered at 3–37 Hz. For each contact, either the low-frequency (dystonia) or beta (PD) spectral peak were obtained and used to set the central frequency for online filtering ± 3 Hz (Fig. 2). Amplitude envelopes were obtained from the filtered LFPs, and a threshold was defined around ~50–60% of the total amplitude. Stimulation was switched on every time a burst was detected, and stimulation lasted until the burst ended. A ramping period of 250 ms was used every time the stimulation was either switched on or off, in order to avoid stimulation-induced capsular/visual responses. In the dystonia patient, aDBS recordings were conducted from each contact combination (2 left, 2 right, total 4), whereas in the PD patient the contacts with the most prominent beta peak per hemisphere were used. Intraoperative recordings lasted approximately 200 s per condition (sampling rate = 1000 Hz), and started with NoStim due to a potential incomplete wash-out effect by stimulation. During the PD trial, a clinical assessment using a short version of the UPDRS (finger tapping, hand movements, pronation-supination, rest tremor and postural tremor) was videotaped on each condition and blindly scored afterwards by a movement disorders specialist. In the Dystonia-GPi patient, we only focused on the presence of possible side effects derived from aDBS, due to the limited intraoperative recording time and the delayed clinical response in dystonia to DBS.

2.3.2. Stimulation fraction adaptive DBS

The total amount of time each aDBS trial lasted was divided into smaller segments (~20 for each recording). For each segment, the total time fraction that the stimulation was ON was determined, and
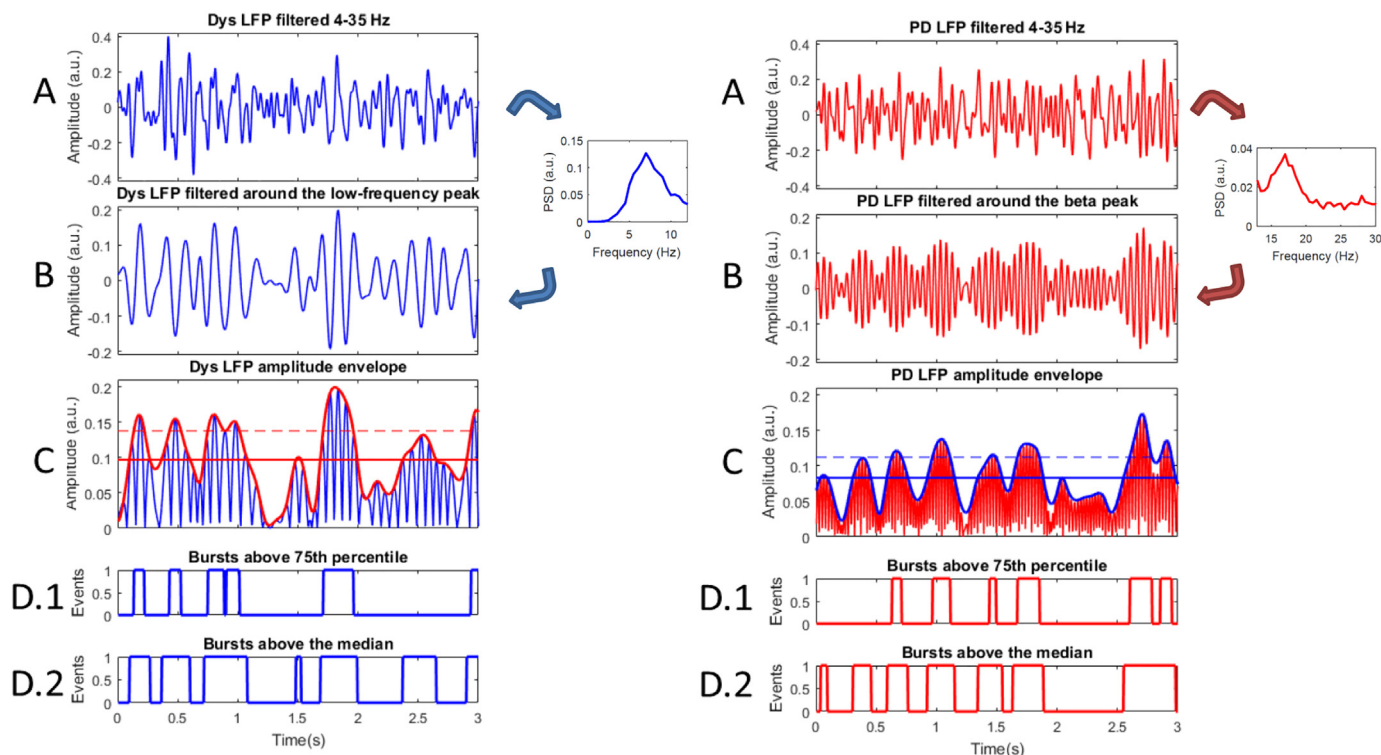
Fig. 1. Example of the determination of low-frequency bursts and beta bursts and their relationship with the bursting behavior of the LFP of one dystonia and one PD patient, respectively. A) LFPs filtered around 4–35 Hz. B) LFPs were bandpass filtered around the frequency peak. In this example the left LFP was filtered around ± 7 Hz, and the right peak was filtered around 20 Hz. C) The signal envelope was obtained using the modulus of the Hilbert transformed LFP. The continuous line indicate the median of the amplitude and the dashed line indicates the 75th percentile. D) Burst count D.1) Based on the moments that the power remains above the 75th percentile. D.2) Based on the moments that the power remains above the median.

expressed as a stimulation fraction of that segment. The stimulation fraction is directly proportional to the amount of LF or beta amplitude detected (i.e. more amplitude above the threshold equals a higher stimulation fraction).

2.4. Statistical analysis

Statistical comparisons were performed between the Dystonia-GPi and the PD-GPi data, and between the PD-GPi and PD-STN data. All
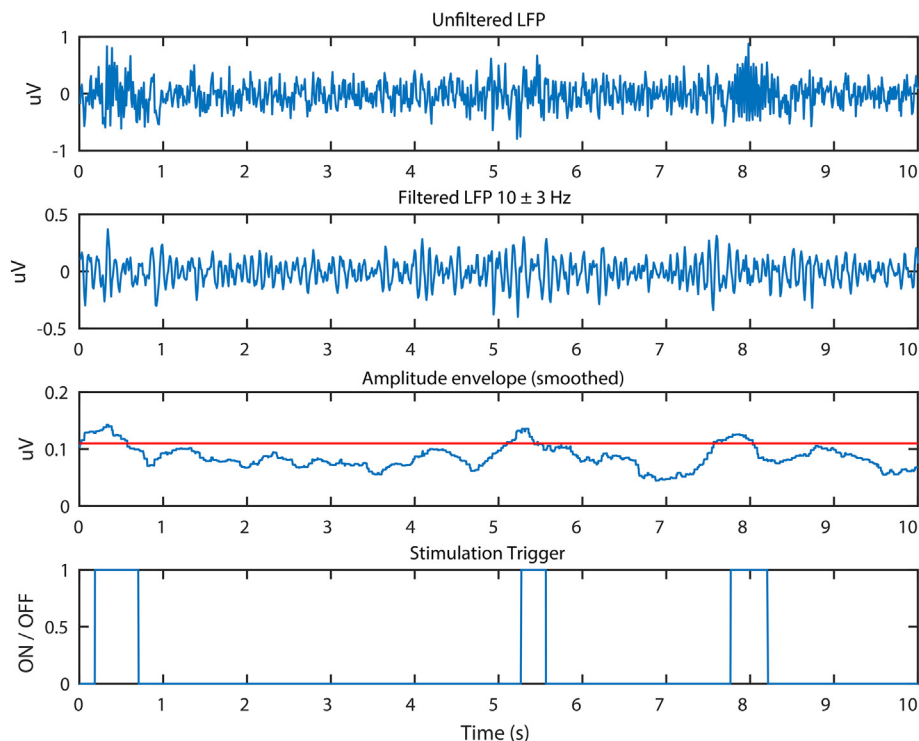

Fig. 2. Example of the application of adaptive DBS based on low-frequency oscillations in dystonia. Upper row: bipolar local field potential (LFP) derived from the internal part of the Globus Pallidus (GPi) filtered between 3 and 37 Hz. Second row: LFP filtered between the peak in low-frequency oscillations ± 3 Hz (i.e. 10 ± 3 Hz). Third row: average low-frequency amplitude envelope over 400 ms moving average. The red line depicts the threshold determined for providing stimulation, i.e. when the amplitude is exceeding the red line, stimulation is provided. Lower row: Stimulation trigger showing at which moments high-frequency stimulation was provided. (For interpretation of the references to colour in this figure legend, the reader is referred to the web version of this article.)

data were visually inspected for normality using Q-Q plots. The PSD estimates obtained with Welch's method were tested using a cluster based two-tailed permutation *t*-test for independent samples using a Montecarlo approach with 3000 permutations. The alpha level for the cluster threshold was set at 0.05 and an alpha of 0.025 to control the false alarm rate. CoV across frequency bands, burst amplitude and length, and burst amplitude and length quartiles were tested using a two-way independent ANOVA test (4 × 2 design for CoV and burst amplitude and length quartiles, and 9 × 2 design for burst duration and amplitude intervals).

For the aDBS data, correlations between fraction of stimulation and time were conducted using Spearman's rho.

3. Results

No significant differences were shown in the PSD estimates, CoV or burst characteristics between PD-STN and PD-GPi datasets.

3.1. Power spectral density

The PSD estimates of Dystonia-GPi and PD-GPi showed two significantly different regions. (Fig. 3). The first was located at 9–10.5 Hz (cluster $t = 9.7542$, p corrected $= 0.0427$) and the second at 15.5–20 Hz (cluster $t = -28.4216$, p corrected $= 0.0177$).
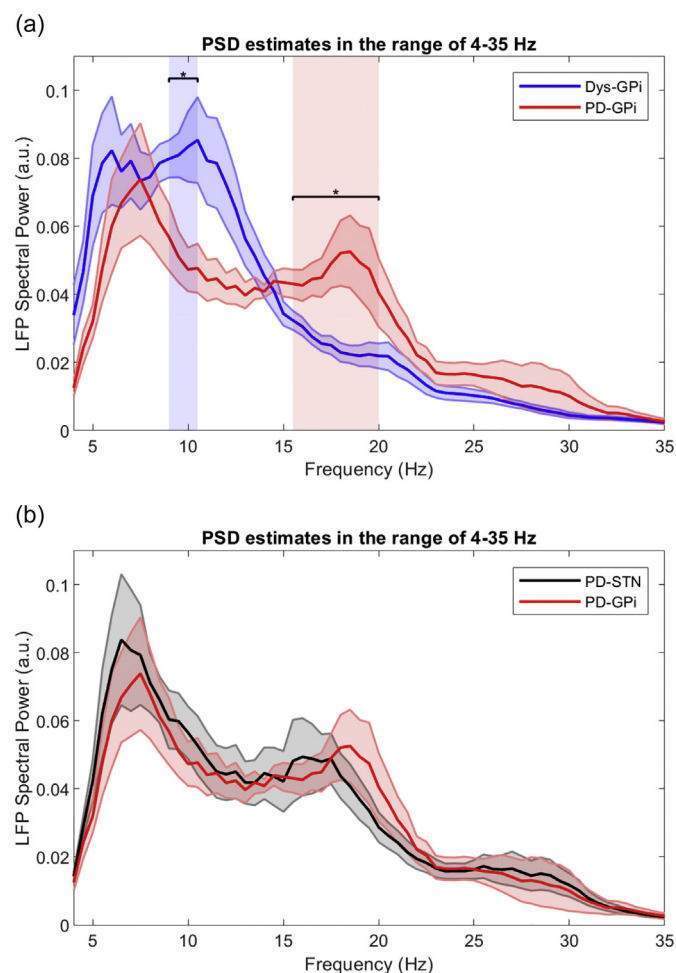
(a)

(b)

Fig. 3. *Upper panel* Averaged resting state LFP PSD estimates for Dystonia-GPi (blue) and PD-GPi (red) ± SEM. Shaded areas indicate clusters that significantly differed (Shaded blue for low frequency and shaded red for beta frequency bands). *Lower panel.* Same comparison for PD-STN and PD-GPi. (For interpretation of the references to colour in this figure legend, the reader is referred to the web version of this article.)

3.2. Coefficient of variation

The CoV in Dystonia-GPi (0.63 ± 0.01) was significantly higher than in PD (0.57 ± 0.01), main effect: F(1,87) = 4.9834, $p = 0.0284$ (Fig. 4). Differences in frequency band (F(3,87) = 0.95, $p = 0.41$), and interaction between disease and frequency band (F(3, 87) = 0.42, $p = 0.73$) were not significant.

3.3. Bursts

In line with previous literature (Tinkhauser et al., 2017a, b), the results of the burst analysis using a 75th-percentile threshold were reported. Statistical results are summarized in Table 3. Complementary burst analyses were performed across different thresholds for validation (50th, 55th, 60th, 65th, 70th,80th, 85th, and 90th percentile). Briefly, analyses of amplitude showed significantly higher LF burst amplitudes in Dystonia-GPi (Fig. 5) and significantly higher beta burst amplitudes in PD-GPi (Fig. 6). Dystonic LF bursts were more prominent in the highest LF amplitude quartile, while parkinsonian LF bursts were more prominent in the lowest LF amplitude quartiles. On the other hand, dystonic beta bursts were more prominent in the lowest beta amplitude quartile, while parkinsonian beta bursts were more prominent in the highest beta amplitude quartile. These results remained significant across virtually all thresholds when tested for both LF bursts and beta bursts. Differences in burst length were significant neither for LF bursts nor beta bursts. A thorough visual description of the different analysis using increasing thresholds can be found in the Supplementary Figs. 2–17.

3.4. Adaptive DBS

LFPs used for feedback in the closed-loop system of aDBS were filtered around 10 ± 3 Hz in Dystonia-GPi and a 18 ± 3 Hz in PD-GPi. The average stimulation voltage was matched up with the therapeutic voltage used in practice, being in dystonia 1 V and 2.3 V in PD. GPi-aDBS was well tolerated in both patients and only elicited transient contractions at supraliminal voltages in the extremities contralateral to the stimulation side. aDBS was provided in such a way that it stimulated on average 34% of the time in the dystonia patient and 26.7% of the time in PD. From the beginning to the end of the aDBS condition, despite fixed thresholds, the stimulation fraction dropped significantly, both in PD (ρ = −0.42, $p = 0.04$) and dystonia (ρ = −0.45, p = 0.04) (Fig. 7 c/d). The UPDRS subscores for the PD patient were 11 during OFF, 7 under cDBS (37% improvement) and 4 under aDBS (64% improvement). Even though no systematic clinical evaluation in the dystonia aDBS trial was performed, the patient reported a subjective symptom relief under cDBS/aDBS. However, as expected, no visual differences were perceived by the research team at the moment of cDBS/aDBS application, most probably due to the brevity of the recording.

4. Discussion

In the present study, we found that the characteristics of pallidal LF and beta bursts are similar between the parkinsonian GPi and STN, whereas significant differences were found in the amplitude/power of LF and beta oscillations between the parkinsonian and the dystonic GPi. These characteristics provided us a rationale to trial aDBS based on the LF burst amplitude in Dystonia-GPi or beta burst amplitude in PD-GPi.

4.1. Significance of disease burst profiles

Similar to other pathophysiological findings in movement disorders (Cilia et al., 2014; Shawky, 2014; Taylor et al., 2016) disease-related increased oscillations are not a sine qua non (Wang et al., 2016). Nevertheless, differences in basal-ganglia oscillatory resting spectral
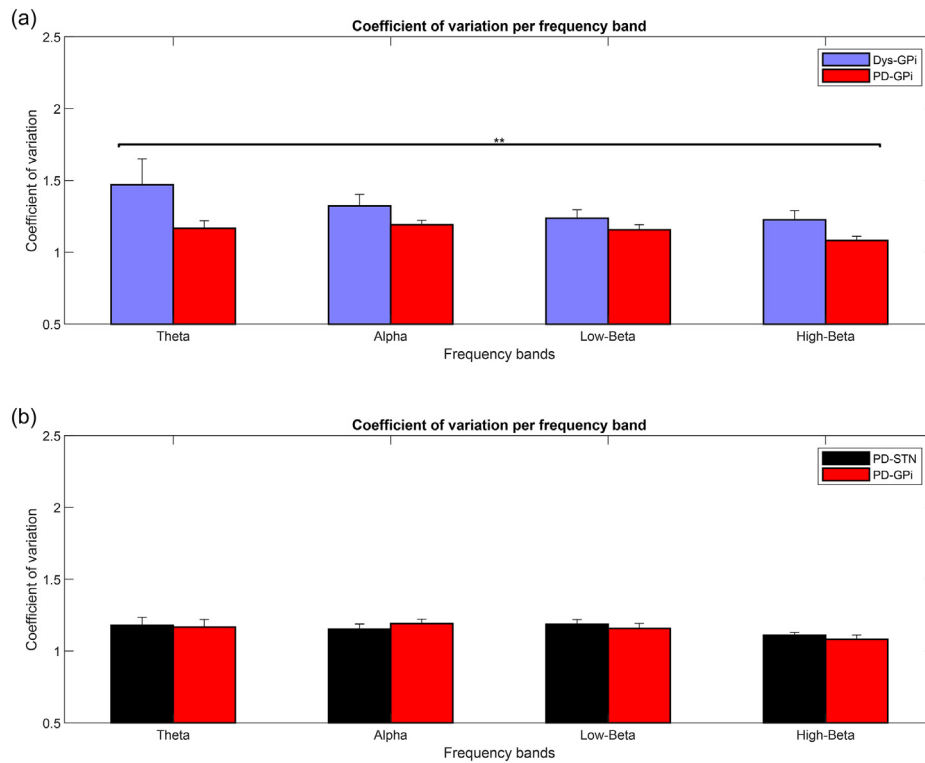
(a)

(b)

Fig. 4. A) Coefficient of variation (CoV, standard deviation (σ)/mean (μ)) of Dystonia-GPi and PD-GPi LFPs across different frequency bands (theta: 4–8 Hz, alpha: 8–12 Hz, low beta: 13–20 Hz, high beta: 21–35 Hz) and B) CoV of PD-STN and PD-GPi LFPs. ** = $p < 0.05$.
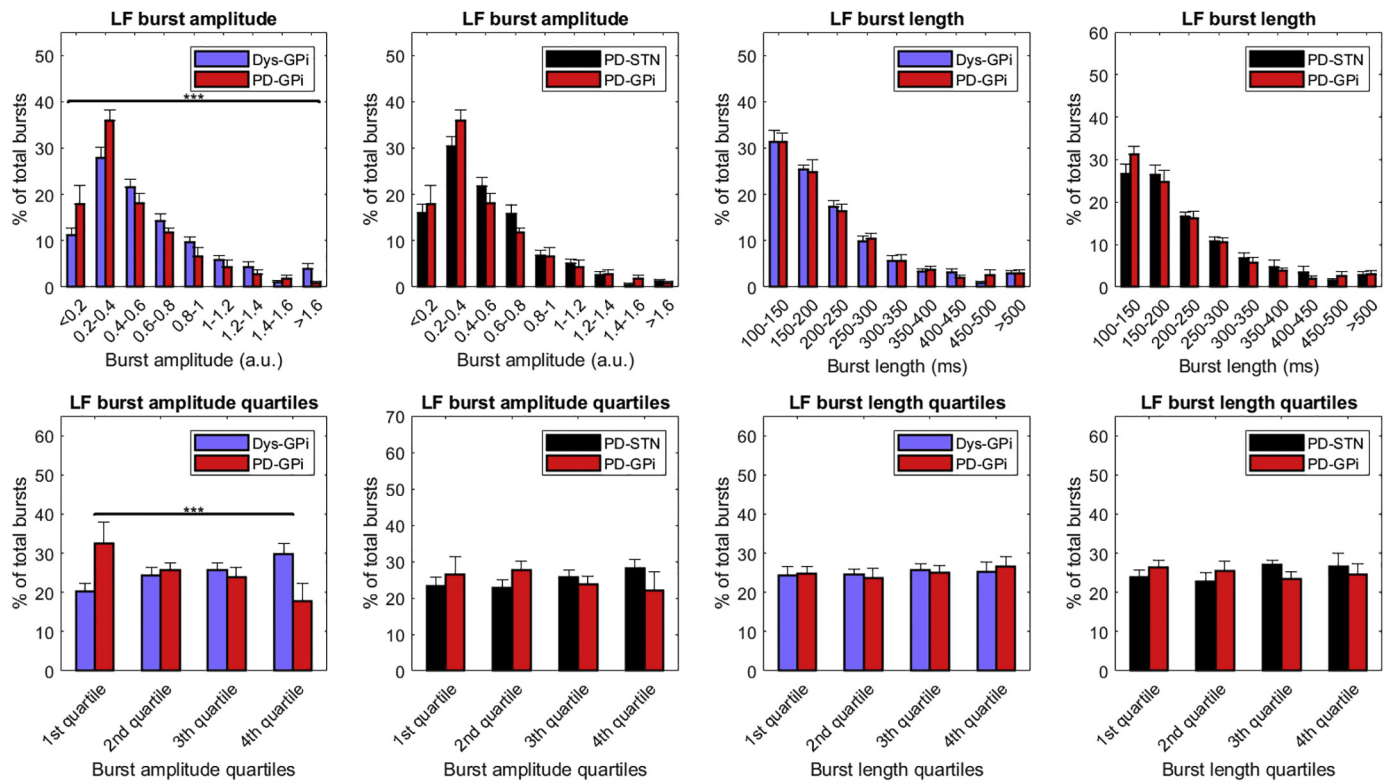

Fig. 5. Comparison of LF burst characteristics between dystonia-GPi and PD-GPi, and between PD-STN and PD-GPi. *Upper row:* LF burst amplitude and length divided on intervals. *Lower row:* LF burst amplitude and length divided on quartiles. *Left columns:* LF burst amplitude. *Right columns:* LF burst length. ***Significant effect of the interaction.
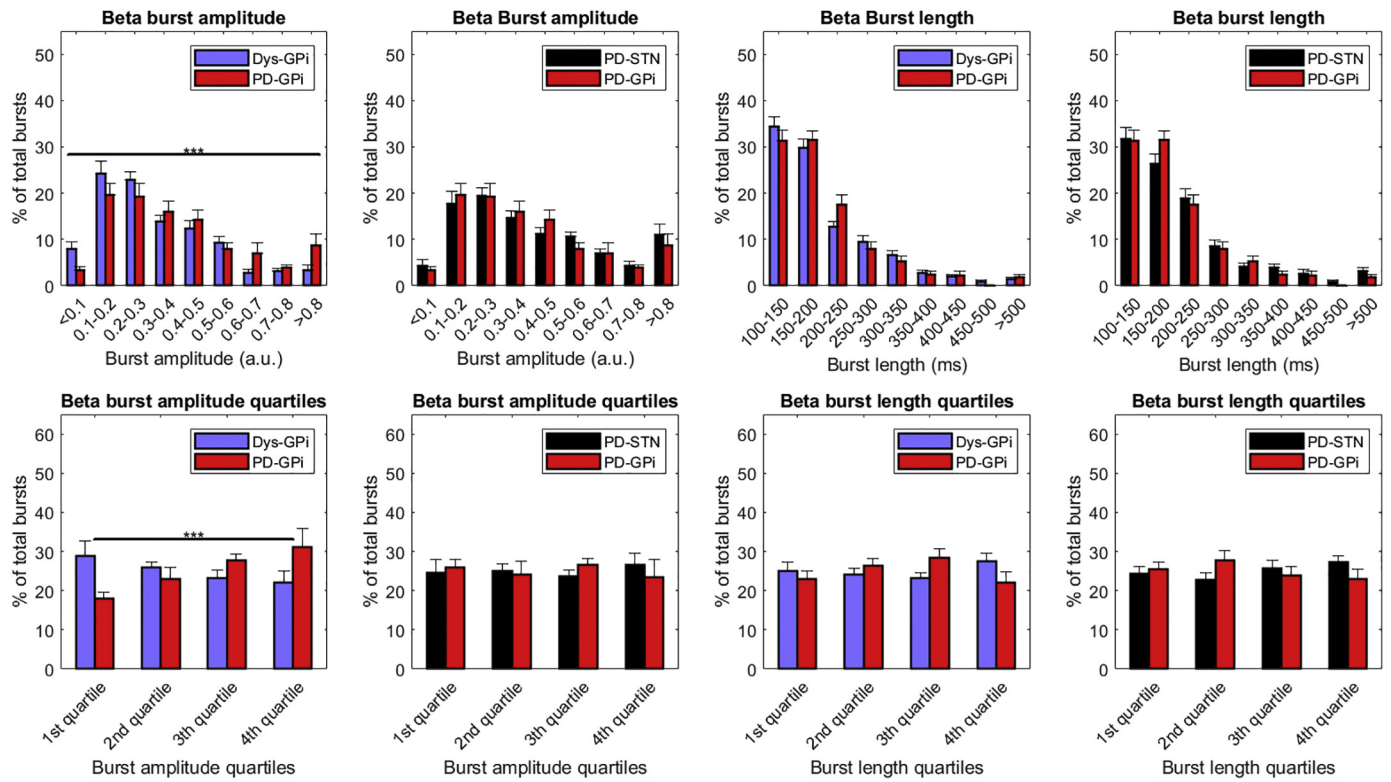
Fig. 6. Comparison of beta burst characteristics between dystonia-GPi and PD-GPi, and between PD-STN and PD-GPi. *Upper row:* beta burst amplitude and length divided on intervals. *Lower row*: beta burst amplitude and length divided on quartiles. *Left columns:* beta burst amplitude. *Right columns:* beta burst length. ***Significant effect of the interaction.

Table 3
Statistical results of burst analysis. PD = Parkinson's disease, Dys = dystonia, GPi = internal globus pallidus, LF = low frequency, SEM = standard error of the mean.

Variables	Mean percentage (% ± SEM)	Interaction effect (degrees of freedom)	Significance (p)
LF burst amplitude			
Intervals		F(8,197) = 3.5181	0.0008
Quartiles		F(3,87) = 5.8939	0.0011
-Dystonia-GPi	Q1: 20.18 (2.18)		
	Q4: 29.82 (2.76)		
-PD-GPi	Q1: 32.51 (5.50)		
	Q4: 17.81 (4.65)		
Beta burst amplitude			
Intervals		F(8,197) = 2.2185	0.0280
Quartiles		F(3,87) = 4.3854	0.0066
-Dystonia-GPi	Q1: 28.97 (3.75)		
	Q4: 22.08 (2.84)		
-PD-GPi	Q1: 22.08 (1.70)		
	Q4: 31.21 (4.70)		
LF burst length			
Intervals		F(8,197) = 0.2172	0.9875
Quartiles		F(3,87) = 0.0916	0.9645
-Dystonia-GPi	Q1: 24.40(2.16)		
	Q4: 25.35(2.43)		
-PD-GPi	Q1: 24.73 (1.89)		
	Q4: 26.51 (2.52)		
Beta burst length			
Intervals		F(8,197) = 1.2648	0.2645
Quartiles		F(3,87) = 2.5687	0.0601
-Dystonia-GPi	Q1: 25.03 (2.34)		
	Q4: 27.56 (1.90)		
-PD-GPi	Q1: 23.02 (2.08)		
	Q4: 22.14 (2.60)		

power of PD and dystonia have been consistently described (Geng et al., 2017; Silberstein et al., 2003; Tang et al., 2007; Weinberger et al., 2012). This indicates a more prominent role of certain oscillations in the pathology of movement disorders and further supports their use for aDBS. In this article, we found that those characteristic patterns are mainly caused by differences in burst amplitude. Wang et al. also found that the main difference between parkinsonian and dystonic pallidal beta bursts is related to their amplitude (Wang et al., 2018). The presence of similar burst characteristics between the parkinsonian GPi and STN further supports this theory. In previous articles (Tinkhauser et al., 2017a, b), the burst characteristics were assessed in response to treatment, either stimulation or levodopa administration, using a common threshold between conditions. This raises the question about which burst characteristics (e.g. burst length) are more dependent to treatment response. During our aDBS trials based on LF and beta amplitude, we found a significant reduction in the fraction of stimulation over time. This indicates that burst length was also decreased (bursts remained above the threshold to trigger stimulation for less time). The clear correlation of amplitude and length (Supplementary Fig. 18) could explain why modifying one of both parameters can have repercussions for the other. Occasionally, brief periods of intense generalized dystonic activity are registered on the bipolar LFP recordings (Chen et al., 2006); this might explain the increased CoV in dystonia, showed in this article. The presence of (less prominent) LF oscillations in PD might be partially explained by the co-occurrence of dystonic symptoms that some PD patients experience (Tolosa and Compta, 2006).

Oscillations within the basal ganglia and cortical structures have been widely related to (patho)physiological motor performance (Lanciego et al., 2012). Beta oscillations are involved in maintaining a resting state, as they decrease during movement performance (Jurkiewicz et al., 2006). Analogously, LF have been associated with movement ideation and performance (Popovych et al., 2016).
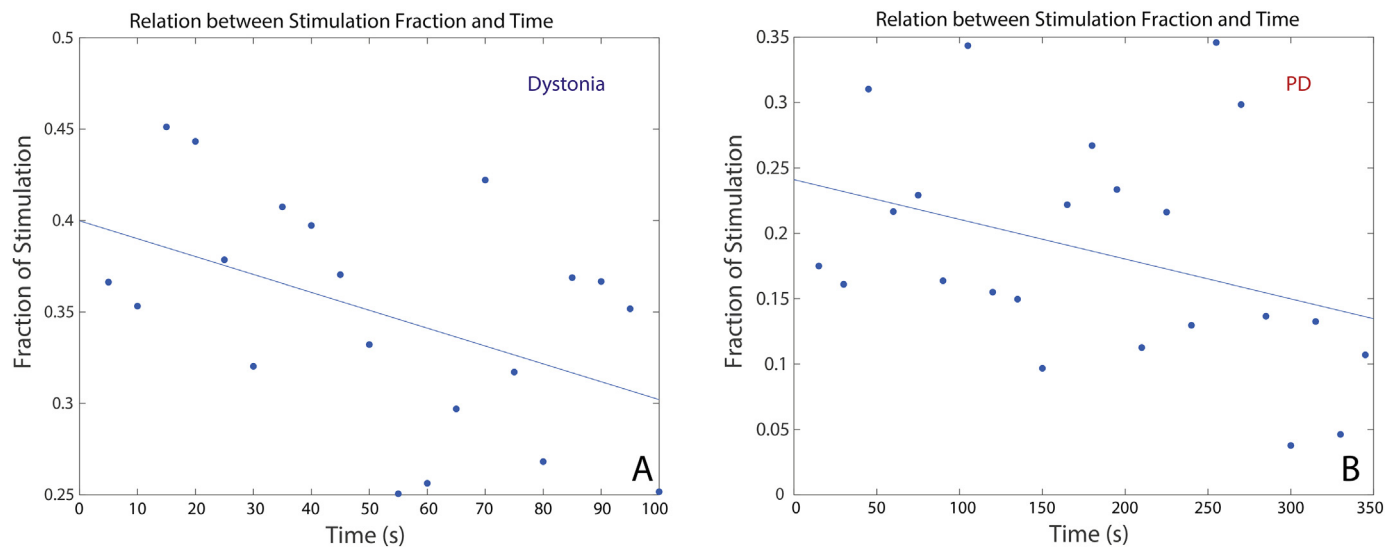
Fig. 7. A. Relation between the fraction of time that stimulation is turned on (Fraction of Stimulation) and the advancement of the application of aDBS in a dystonia-GPi patient, together with its least square line. B. Similar relation in a PD-GPi patient.

Therefore, the presence of subcortical exaggerated beta oscillations shown in PD, or LF oscillations in dystonia, might indicate that affected neuronal networks are under a oscillatory state that aberrantly promotes either maintenance of the resting state (hypokinetic) or the performance of movements (hyperkinetic), respectively.

4.2. Rationale for the implementation of aDBS to dystonia

Despite its proven effectiveness, cDBS still presents certain limitations. Given the correlation of LF with phasic dystonic symptoms (Barow et al., 2014; Liu et al., 2006; Neumann et al., 2017), aDBS devices based on LF amplitude might be able to reflect the real-time status of, at a minimum, mobile dystonia. The application of dynamic physiomarkers for DBS in dystonia would allow future devices to dynamically modulate stimulation and possibly, use LF as an adjuvant to facilitate the challenging endeavor of (initial) programming (Picillo et al., 2016). In this study, we demonstrate that the LF have a dynamic behavior over time, coming in the form of short-lived high-amplitude bursts, similarly to their beta counterpart in PD (Tinkhauser et al., 2017a). This fact provides a rationale for an aDBS ON/OFF intermittent approach based on the setting of an amplitude threshold for LF, in order to selectively modulate high-amplitude bursts.

4.3. Testing aDBS in the GPi

To our knowledge, this is the first time that aDBS has been trialed in the GPi of both a PD and a dystonia patient. The particular presence of beta oscillations in our PD patient and their subsequent modulation by aDBS suggests that adaptive basal ganglia beta modulation might also be achieved from the GPi, in which clinical response was obtained with both cDBS and aDBS. We also showed that aDBS in dystonia based on the amplitude of LF bursts is technically possible and well tolerated in an experimental setting. Even though a visible clinical response could not be demonstrated due to the short duration of the setting, the reduction of LF burst amplitude/duration over time, even when stimulation is not continuous, might illustrate a form of short-term plasticity (Fenoy et al., 2014). At present however, we cannot yet say whether there would be any clinical benefit since a response in dystonia to DBS is usually delayed (Picillo et al., 2016). Long-term recordings (Swann et al., 2018), using an implantable device capable of stimulating and sensing neuronal activity, will be able to evaluate the clinical response of dystonia to aDBS and its 'neurophysiological fingerprint' over time.

5. Limitations

The main limitation of this study is the short intraoperative time in which we were able to perform the recordings. In many centers, DBS system implantation (electrodes and battery) takes place on the same day, which allows patients to quickly move forward to the recovery period. This gives a small intraoperative window of opportunity to perform the recordings. We also performed some recordings during battery replacement operations, which have the advantage of bypassing the stun-effect caused by electrode implantation. In light of the fact that recording from healthy subjects is not viable due to the invasive nature of the procedure, the comparison of normalized signals between diseases, or the use of pre- and post-treatment recordings, seem to be reliable methods to determine which features are related to each disease. Also, signals were normalized to account for voltage differences between electrode positions. The limited number of patients included are mostly due to the intrinsic limitations of this type of intra-operative measurements, especially on interventions on dystonia patients without general anesthesia. However, even with this limitation, a significant difference in burst amplitude was found, which together with the literature available, likely indicates a real difference in amplitude between oscillations of PD and dystonia.

6. Conclusion

This study shows that the characteristics of high-amplitude short-lived bursts are similar between the parkinsonian GPi and STN, but different in the dystonic and parkinsonian GPi, giving the basis for formal trialing of GPi aDBS in dystonia and PD. Also, it indicates that applying aDBS in the GPi of both dystonia and PD using a phasic ON/OFF burst approach is safe and well tolerated. Chronic studies will be able to determine the clinical efficacy of aDBS in dystonia.

Supplementary data to this article can be found online at https://doi.org/10.1016/j.nbd.2018.09.014.

Conflict of interest

All the authors declare no conflict of interest.

('*Hersenstichting Nederland*'), the National Mexican Council of Science and Technology (*CONACYT)* and the University of Groningen/ University Medical Center Groningen (*RuG/UMCG*). G.T. is supported by a grant from the Swiss Parkinson Association. S Little is personally supported by the Wellcome Trust (105804/Z/14/Z).

Author contributions

References

Arlotti, M., Marceglia, S., Foffani, G., Volkmann, J., Lozano, A.M., Moro, E., Cogiamanian, F., Prenassi, M., Bocci, T., Cortese, F., Rampini, P., Barbieri, S., Priori, A., 2018. Eight-hours adaptive deep brain stimulation in patients with Parkinson disease. Neurology. https://doi.org/10.1212/WNL.0000000000005121.

Balint, B., Bhatia, K.P., 2014. Dystonia: an update on phenomenology, classification, pathogenesis and treatment. Curr. Opin. Neurol. 27, 468–476. https://doi.org/10.1097/WCO.0000000000000114.

Barow, E., Neumann, W.-J., Brucke, C., Huebl, J., Horn, A., Brown, P., Krauss, J.K., Schneider, G.-H., Kuhn, A.A., 2014. Deep brain stimulation suppresses pallidal low frequency activity in patients with phasic dystonic movements. Brain 137, 3012–3024. https://doi.org/10.1093/brain/awu258.

Beudel, M., Brown, P., 2016. Adaptive deep brain stimulation in Parkinson's disease. Parkinsonism Relat. Disord. 22https://doi.org/10.1016/j.parkreldis.2015.09.028. Suppl 1, S123-6.

Brown, P., Oliviero, A., Mazzone, P., Insola, A., Tonali, P., Di Lazzaro, V., 2001. Dopamine Dependency of Oscillations between Subthalamic Nucleus and Pallidum in Parkinson's Disease. 21. pp. 1033–1038.

Chen, C.C., Kühn, A.A., Hoffmann, K.T., Kupsch, A., Schneider, G.H., Trottenberg, T., Krauss, J.K., Wöhrle, J.C., Bardinet, E., Yelnik, J., Brown, P., 2006. Oscillatory pallidal local field potential activity correlates with involuntary EMG in dystonia. Neurology 66, 418–420. https://doi.org/10.1212/01.wnl.0000196470.00165.7d.

Chiken, S., Nambu, A., 2016. Mechanism of deep brain stimulation: inhibition, excitation, or disruption? Neuroscientist 22, 313–322. https://doi.org/10.1177/1073858415581986.

Chu Chen, C., Kühn, A.A., Trottenberg, T., Kupsch, A., Schneider, G.H., Brown, P., 2006. Neuronal activity in globus pallidus interna can be synchronized to local field potential activity over 3-12 Hz in patients with dystonia. Exp. Neurol. 202, 480–486. https://doi.org/10.1016/j.expneurol.2006.07.011.

Cilia, R., Reale, C., Castagna, A., Nasca, A., Muzi-Falconi, M., Barzaghi, C., Marzegan, A., Granata, M., Marotta, G., Sacilotto, G., Vallauri, D., Pezzoli, G., Goldwurm, S., Garavaglia, B., 2014. Novel DYT11 gene mutation in patients without dopaminergic deficit (SWEDD) screened for dystonia. Neurology 83, 1155–1162. https://doi.org/10.1212/WNL.0000000000000821.

Fenoy, A.J., Goetz, L., Chabardès, S., Xia, Y., 2014. Deep brain stimulation: are astrocytes a key driver behind the scene? CNS Neurosci. Ther. 20, 191–201. https://doi.org/10.1111/cns.12223.

Foncke, E.M.J., Bour, L.J., Speelman, J.D., Koelman, J.H.T.M., Tijssen, M.A.J., 2007. Local field potentials and oscillatory activity of the internal globus pallidus in myoclonus-dystonia. Mov. Disord. 22, 369–376. https://doi.org/10.1002/mds.21284.

Geng, X., Zhang, J., Jiang, Y., Ashkan, K., Foltynie, T., Limousin, P., Zrinzo, L., Green, A., Aziz, T., Brown, P., Wang, S., 2017. Comparison of oscillatory activity in subthalamic nucleus in Parkinson's disease and dystonia. Neurobiol. Dis. 98, 100–107. https://doi.org/10.1016/j.nbd.2016.12.006.

Jimenez-Shahed, J., Telkes, I., Viswanathan, A., Ince, N.F., 2016. GPi oscillatory activity differentiates tics from the Resting State, voluntary movements, and the unmedicated Parkinsonian State. Front. Neurosci. 10 (436). https://doi.org/10.3389/fnins.2016.00436.

Jurkiewicz, M.T., Gaetz, W.C., Bostan, A.C., Cheyne, D., 2006. Post-movement beta rebound is generated in motor cortex: evidence from neuromagnetic recordings. NeuroImage 32, 1281–1289. https://doi.org/10.1016/j.neuroimage.2006.06.005.

Lanciego, J.L., Luquin, N., Obeso, J.A., 2012. Functional neuroanatomy of the basal ganglia. Cold Spring Harb. Perspect. Med. https://doi.org/10.1101/cshperspect.a009621.

Little, S., Pogosyan, A., Kuhn, A.A., Brown, P., 2012. Beta band stability over time correlates with Parkinsonian rigidity and bradykinesia. Exp. Neurol. 236, 383–388. https://doi.org/10.1016/j.expneurol.2012.04.024.

Little, S., Pogosyan, A., Neal, S., Zavala, B., Zrinzo, L., Hariz, M., Foltynie, T., Limousin, P., Ashkan, K., Fitzgerald, J., Green, A.L., Aziz, T.Z., Brown, P., 2013. Adaptive deep brain stimulation in advanced Parkinson disease. Ann. Neurol. 74, 449–457. https://doi.org/10.1002/ana.23951.

Little, S., Beudel, M., Zrinzo, L., Foltynie, T., Limousin, P., Hariz, M., Neal, S., Cheeran, B., Cagnan, H., Gratwicke, J., Aziz, T.Z., Pogosyan, A., Brown, P., 2016. Bilateral adaptive deep brain stimulation is effective in Parkinson's disease. J. Neurol. Neurosurg. Psychiatry 87, 717–721. https://doi.org/10.1136/jnnp-2015-310972.

Liu, X., Yianni, J., Wang, S., Bain, P.G., Stein, J.F., Aziz, T.Z., 2006. Different mechanisms may generate sustained hypertonic and rhythmic bursting muscle activity in idiopathic dystonia. Exp. Neurol. 198, 204–213. https://doi.org/10.1016/j.expneurol.2005.11.018.

Moro, E., Lereun, C., Krauss, J.K., Albanese, A., Lin, J.P., Walleser Autiero, S., Brionne, T.C., Vidailhet, M., 2017. Efficacy of pallidal stimulation in isolated dystonia: a systematic review and meta-analysis. Eur. J. Neurol. 24, 552–560. https://doi.org/10.1111/ene.13255.

Neumann, W.-J., Degen, K., Schneider, G.-H., Brücke, C., Huebl, J., Brown, P., Kühn, A.A., 2016. Subthalamic synchronized oscillatory activity correlates with motor impairment in patients with Parkinson's disease. Mov. Disord. 31, 1748–1751. https://doi.org/10.1002/mds.26759.

Neumann, W.-J., Horn, A., Ewert, S., Huebl, J., Brücke, C., Slentz, C., Schneider, G.-H., Kühn, A.A., 2017. A localized pallidal physiomarker in cervical dystonia. Ann. Neurol. https://doi.org/10.1002/ana.25095.

Odekerken, V.J.J., Boel, J.A., Schmand, B.A., de Haan, R.J., Figee, M., van den Munckhof, P., Schuurman, P.R., de Bie, R.M.A., 2016. GPi vs STN deep brain stimulation for Parkinson disease: Three-year follow-up. Neurology 86, 755–761. https://doi.org/10.1212/WNL.0000000000002401.

Picillo, M., Lozano, A.M., Kou, N., Munhoz, R.P., Fasano, A., 2016. Programming deep brain stimulation for tremor and dystonia: the Toronto western hospital algorithms. Brain Stimul. 9, 438–452. https://doi.org/10.1016/j.brs.2016.02.003.

Piña-Fuentes, D., Little, S., Oterdoom, M., Neal, S., Pogosyan, A., Tijssen, M.A.J., van Laar, T., Brown, P., van Dijk, J.M.C., Beudel, M., 2017. Adaptive DBS in a Parkinson's patient with chronically implanted DBS: a proof of principle. Mov. Disord. 32. https://doi.org/10.1002/mds.26959.

Piña-Fuentes, D., Beudel, M., Little, S., Van Zijl, J., Elting, J.W., Oterdoom, D.L.M., Van Egmond, M.E., Van Dijk, J.M.C., 2018. Toward adaptive deep brain stimulation for dystonia. Neurosurg. Focus. 45, 1–8. https://doi.org/10.3171/2018.5.FOCUS18155.

Popovych, S., Rosjat, N., Toth, T.I., Wang, B.A., Liu, L., Abdollahi, R.O., Viswanathan, S., Grefkes, C., Fink, G.R., Daun, S., 2016. Movement-related phase locking in the delta-theta frequency band. NeuroImage 139, 439–449. https://doi.org/10.1016/j.neuroimage.2016.06.052.

Rosa, M., Arlotti, M., Marceglia, S., Cogiamanian, F., Ardolino, G., Di Fonzo, A., Lopiano, L., Scelzo, E., Merola, A., Locatelli, M., Rampini, P.M., Priori, A., 2017. Adaptive deep brain stimulation controls levodopa-induced side effects in Parkinsonian patients. Mov. Disord. 32, 628–629. https://doi.org/10.1002/mds.26953.

Shawky, R.M., 2014. Reduced penetrance in human inherited disease. Egypt. J. Med. Hum. Genet. 15, 103–111. https://doi.org/10.1016/j.ejmhg.2014.01.003.

Silberstein, P., Kuhn, A.A., Kupsch, A., Trottenberg, T., Krauss, J.K., Wohrle, J.C., Mazzone, P., Insola, A., Di Lazzaro, V., Oliviero, A., Aziz, T., Brown, P., 2003. Patterning of globus pallidus local field potentials differs between Parkinson's disease and dystonia. Brain 126, 2597–2608. https://doi.org/10.1093/brain/awg267.

Starr, P.A., Rau, G.M., Davis, V., Marks, W.J.J., Ostrem, J.L., Simmons, D., Lindsey, N., Turner, R.S., 2005. Spontaneous pallidal neuronal activity in human dystonia: comparison with Parkinson's disease and normal macaque. J. Neurophysiol. 93, 3165–3176. https://doi.org/10.1152/jn.00971.2004.

Swann, N.C., de Hemptinne, C., Miocinovic, S., Qasim, S., Ostrem, J.L., Galifianakis, N.B., Luciano, M.S., Wang, S.S., Ziman, N., Taylor, R., Starr, P.A., 2018. Chronic multisite brain recordings from a totally implantable bidirectional neural interface: experience in 5 patients with Parkinson's disease. J. Neurosurg. 128, 605–616. https://doi.org/10.3171/2016.11.JNS161162.

Tang, J.K.H., Moro, E., Mahant, N., Hutchison, W.D., Lang, A.E., Lozano, A.M., Dostrovsky, J.O., 2007. Neuronal firing rates and patterns in the globus pallidus internus of patients with cervical dystonia differ from those with Parkinson's disease. J. Neurophysiol. 98, 720–729. https://doi.org/10.1152/jn.01107.2006.

Taswell, C., 2000. The what, how, and why of wavelet shrinkage denoising. Comput. Sci. Eng. 2, 12–19. https://doi.org/10.1109/5992.841791.

Taylor, S., Gafton, J., Shah, B., Pagano, G., Chaudhuri, K.R., Brooks, D.J., Pavese, N., 2016. Progression of nonmotor symptoms in subgroups of patients with non-dopamine-deficient Parkinsonism. Mov. Disord. 31, 344–351. https://doi.org/10.1002/mds.26456.

Tijssen, M. a, Marsden, J.F., Brown, P., 2000. Frequency analysis of EMG activity in patients with idiopathic torticollis. Brain 123 (4), 677–686. https://doi.org/10.1093/brain/123.4.677. Pt.

Tinkhauser, G., Pogosyan, A., Little, S., Beudel, M., Herz, D.M., Tan, H., Brown, P., 2017a. The modulatory effect of adaptive deep brain stimulation on beta bursts in

Parkinson's disease. Brain 140, 1053–1067. https://doi.org/10.1093/brain/awx010.

Tinkhauser, G., Pogosyan, A., Tan, H., Herz, D.M., Kuhn, A.A., Brown, P., 2017b. Beta burst dynamics in Parkinson's disease OFF and ON dopaminergic medication. Brain 140, 2968–2981. https://doi.org/10.1093/brain/awx252.

Tolosa, E., Compta, Y., 2006. Dystonia in Parkinson's disease. J. Neurol. 253, vii7–vii13. https://doi.org/10.1007/s00415-006-7003-6.

Tsiokos, C., Malekmohammadi, M., Auyong, N., Pouratian, N., 2017. Pallidal low b -low c phase-amplitude coupling inversely correlates with Parkinson disease symptoms. Clin. Neurophysiol. 128, 2165–2178. https://doi.org/10.1016/j.clinph.2017.08.001.

Vidailhet, M., Jutras, M.-F., Grabli, D., Roze, E., 2013. Deep brain stimulation for dystonia. J. Neurol. Neurosurg. Psychiatry 84, 1029–1042. https://doi.org/10.1136/jnnp-2011-301714.

Wang, D.D., de Hemptinne, C., Miocinovic, S., Qasim, S.E., Miller, A.M., Ostrem, J.L., Galifianakis, N.B., San Luciano, M., Starr, P.A., 2016. Subthalamic local field potentials in Parkinson's disease and isolated dystonia: an evaluation of potential biomarkers. Neurobiol. Dis. 89, 213–222. https://doi.org/10.1016/j.nbd.2016.02.015.

Wang, D.D., de Hemptinne, C., Miocinovic, S., Ostrem, J.L., Galifianakis, N.B., San Luciano, M., Starr, P.A., 2018. Pallidal deep-brain stimulation disrupts pallidal beta oscillations and coherence with primary motor cortex in Parkinson's disease. J. Neurosci. 38, 4556–4568. https://doi.org/10.1523/JNEUROSCI.0431-18.2018.

Weinberger, M., Hutchison, W.D., Alavi, M., Hodaie, M., Lozano, A.M., Moro, E., Dostrovsky, J.O., 2012. Oscillatory activity in the globus pallidus internus: comparison between Parkinson's disease and dystonia. Clin. Neurophysiol. 123, 358–368. https://doi.org/10.1016/j.clinph.2011.07.029.